Observation of capillary discharge Ne-like Ar 46.9 nm laser with pre-pulse and main-pulse delay time in the domain of 2–130 μs

Shan Jiang · Yong-peng Zhao · Yao Xie · Miao Xu · Huai-yu Cui · Han Wu · Yang Liu · Qiang Xu · Qi Wang

Abstract We demonstrated the lasing of Ne-like Ar 46.9 nm pumped by capillary discharge with the delay time between pre-pulse and main-pulse ranging from 2 to 130 μs. Results show that the laser output reduced significantly when the delay time is much longer than 12 μs. The temporal evolution of spontaneous radiation emitted from pre-ionized plasma implies that the observed reduction of the laser output is caused by the axial non-uniformity of pre-ionized plasma density and the decrease of pre-ionized plasma density.

1 Introduction

Because of the potential usages in the field of micro-scale and fast process, soft X-ray laser is under investigation by many research groups around the world. In 1994, Rocca et al. [1] demonstrated the first generation of Ne-like Ar 46.9 nm laser by the means of capillary discharge, and this group have done many applications [2–5], such as dense plasma diagnostics and high spatial resolution microscopy. Using the pre-pulse technology [1], the amplitude of laser output can be enhanced, which were also observed by other groups [6–10].

S. Jiang (✉) · Y. Zhao · M. Xu · H. Cui · H. Wu · Y. Liu · Q. Xu · Q. Wang
National Key Laboratory of Science and Technology on Tunable Laser, Harbin Institute of Technology, Harbin 150080, Heilongjiang, China
e-mail: js853261548@gmail.com

Y. Xie
State Key Laboratory of Applied Optics, Changchun Institute of Optics, Fine Mechanics and Physics, Chinese Academy of Sciences, Changchun 130033, Jilin, China

With the pre-pulse, the intensity and the reproducibility of capillary discharge soft X-ray laser could be enhanced. The pre-pulse discharge ionizes the neutral Ar gas filled in the capillary, resulting in a plasma-column consisted of low-ionized Ar before the main current arrives. Rather than breaking through the neutral Ar gas, main current flows through the surface of the conductive plasma column, which reduces the kink instabilities of the compression during the Z-pinch process. In this case, a hot and dense plasma with enhanced axial uniformity can be generated at Z-pinch stagnation, at which moment the gain of Ne-like Ar $3p$–$3s$ $J = 0$–1 is established. Note that an intense and stable laser output can be only achieved with the axially uniform plasma column, which can be generated with a stable compression.
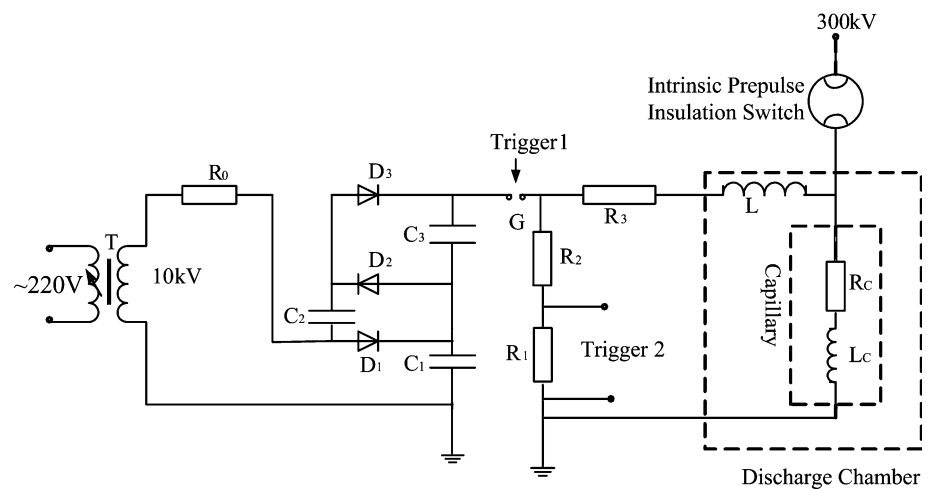
The experimental results show that, the time interval between pre-pulse and main-pulse, called the pre-pulse and main-pulse delay time, plays a key role on the intensity of laser. The pre-ionized plasma states, such as the electron temperature, plasma density, and axial uniformity, evolve with the delay time, which consequentially impact the Z-pinch process when the main-pulse arrives.

Research groups from Israel [6] and Japan [7] have studied the influence of the amplitude of pre-pulse current on 46.9 nm laser. Particularly, the latter [7] group reported that the laser output energy tends to be high and stable with pre-pulse current over 10 A, which agrees with the optimum amplitude range of 10–50 A for laser output described by the former group [6]. In the meanwhile, the group from Israel [8] found that pre-pulse at an amplitude of 100 A could diminish the laser pulse, and the axial flow during the pre-ionization process is attributed to the reduction of lasing intensity. The studies on the pre-pulse and main-pulse delay time were previously reported by Malaysian [9] and Japanese [7] group. Malaysian [10]

group analyzed the laser output versus the pre-pulse and main pulse delay time in the domain of 2–16 μs, which shows that the absorption of the ejected plasma plume and the reduction of pressure is due to the contribution of the variation of lasing intensity [10]. High-speed images of pre-ionized plasma from side view had been taken by Japanese group [7]. The results show that the high and stable laser pulse can only be observed with good axial uniformity of pre-ionized plasma under the delay time less than 30 μs. To date, the research on laser output with the delay time more than 30 μs is still limited.

In this study, capillary discharge soft X-ray laser outputs were obtained with the delay time in the range of 2–130 μs. Spontaneous radiation emitted from pre-ionized plasma had been acquired in temporal and spectral domain, and the influence of the different pre-ionized plasma states over the Z-pinch kinetic process was analyzed.

2 Experimental setup

The experiments were conducted based on a main-pulse generator and a pre-pulse generating circuit. Details on the main-pulse generator have been presented in [11]. Figure 1 presents the diagram of the pre-pulse generating circuit, which is utilized to pre-ionize the Ar gas filled in the capillary. First, a triple voltage circuit is charged by a variable transformer. When trigger 1 signal is received, the gas gap G breaks down and the triple voltage circuit discharges at Ar gas filled in the capillary. While the Ar gas breaks down, the pre-pulse current flows through the capillary. The amplitude of pre-pulse current can be varied by changing the resistance value of R3. Furthermore, while the gas gap G breaks down, trigger 2 is turned on, which is the triggering signal for delay time circuit. After the set delay time, a signal is generated to trigger the main-pulse generator. Eventually, the main pulse is formed and flows
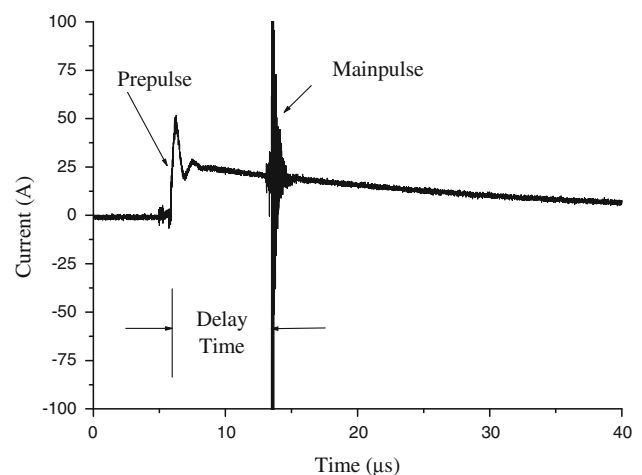

Fig. 2 Current waveform of a typical pre-pulse with main-pulse recorded by oscilloscope

through the pre-ionized plasma inside the capillary. The experiment was conducted with a 3 mm inner diameter and 350-mm-long alumina capillary.

Figure 2 shows the typical current waveforms of pre-pulse current and main-pulse. The main current occurs at about 7 μs after the onset of the pre-pulse current. The amplitude of pre-pulse current is about 25 A, and the waveform is in a shape of exponential decay. The pre-pulse current flows through Ar gas in the capillary, subsequently a pre-ionized plasma column consisted of low-order ions and electrons is created. After the given delay time, main current is generated and flows through the pre-ionized plasma column in the capillary.

To have a better understanding on the kinetic process during the pre-ionization process, the temporal evolution signal and the time-integrated spectra of spontaneous emission from pre-ionized plasma were recorded. We are interested in the relationship between the axial emission and the amplitude of laser output for the delay time in the
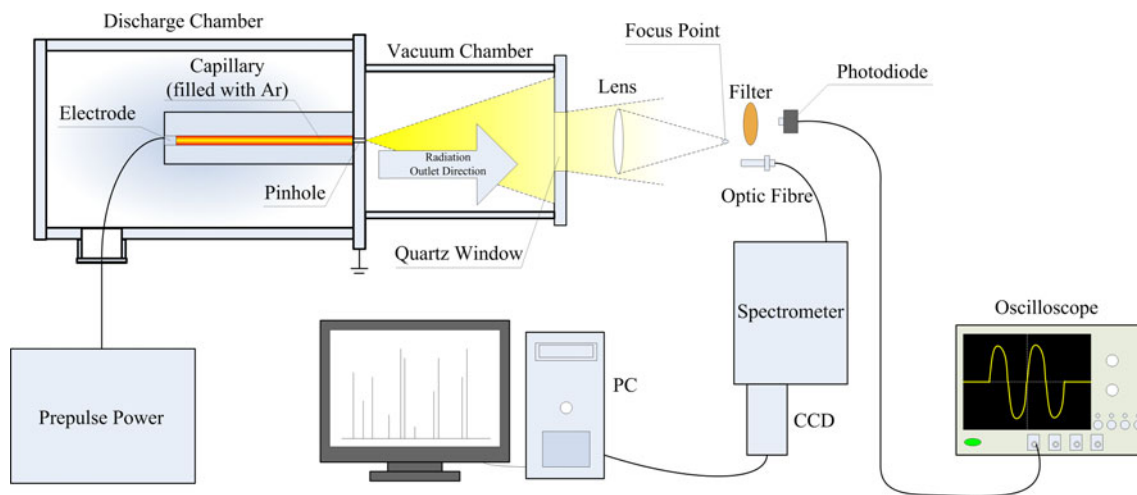
Fig. 3 Experiment setup used to obtain the temporal evolution and the time-integrated spectrum of spontaneous radiation from pre-ionized plasma, either photodiode or optic fibre of spectrometer can be located at the focus point. The photodiode is used to capture the temporal evolution of spontaneous radiation from pre-ionized plasma, and the spectrometer is used to acquire the time-integrated spectrum

range of 2–130 μs. Figure 3 shows the experimental equipments utilized to obtain the temporal evolution signal and the time-integrated spectrum. A quartz window is located at 300 mm away from the pinhole in the direction of radiation outlet. A photodiode (ThorLABs DET10A/M) is mounted at the focus point of the lens outside the quartz window, and used to acquire the temporal evolution of spontaneous radiation. The photodiode has a response time of 1 ns and the spectral response of 150–2,600 nm. The output signal of the photodiode is monitored by a 1 GHz bandwidth digital oscilloscope (Tektronix DPO7104). The temporal evolution of Ar^+ ion and Ar atom emission is measured by using the longpass filters and the photodiode. The time-integrated spectrum is obtained by fixing the optic fibre of a calibrated spectrometer (ANDOR Shamrock SR-750) at the same location as the photodiode, and the spectrum was recorded by CCD (ANDOR NEWTON 971). X-ray diode (XRD) is applied to measure the soft X-ray laser spike signal and background emission emitted from the hot and dense plasma column during the Z-pinch process. The XRD consists of a gold-coated cathode and a metal mesh anode, and a negative bias voltage −600 V is applied on the cathode.

3 Experimental results and discussion

Soft X-ray laser operating on the $3p–3s$ $J = 0–1$ transition of Ne-like Ar is obtained with the main-pulse current, which has an amplitude ranging from 13.6 to 19.0 kA and the 10–90 % rise time of approximately 40 ns. The initial Ar pressure in the capillary is ranging from 14.2 to 22.1 Pa and the peak of pre-pulse current is 20 A. The spectrum
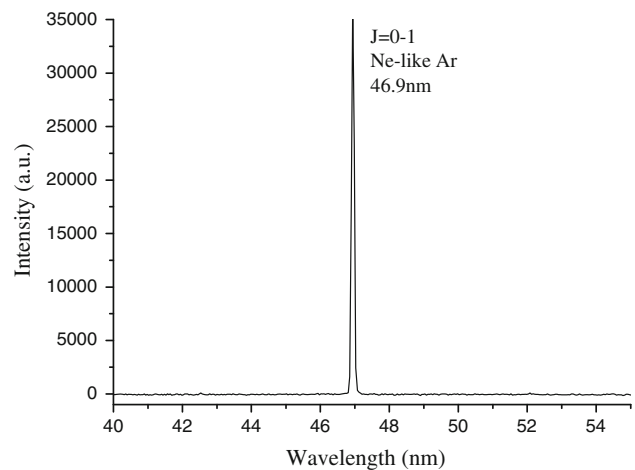
Fig. 4 The time-integrated spectrum obtained from Ar plasma column in 40–55 nm

from Ar plasma is acquired by X-ray spectrometer (McPherson 248/310G) which is presented in Fig. 4. Results shows that the $J = 0–1$ line of Ar IX at 46.9 nm dominates in the spectral domain of 40–55 nm, which indicates that Ne-like Ar 46.9 nm laser has been obtained. Figure 5 presents the typical waveform of main current and soft x-ray emission from plasma column captured by XRD. In the experiment, the quartz window shown in Fig. 3 is replaced by XRD. The laser spike presented in Fig. 5 has an amplitude of 8 V and a duration about 1.7 ns. The spikes appeared after the first one are the reflected signals of laser spike rather than multi-laser pulses. Figure 6 presents the average amplitude of laser output versus delay time. In this experiment, the delay time between pre-pulse and main-pulse is in the domain of 2–132 μs, and the amplitude of main-pulse is about 16.3 kA. The initial
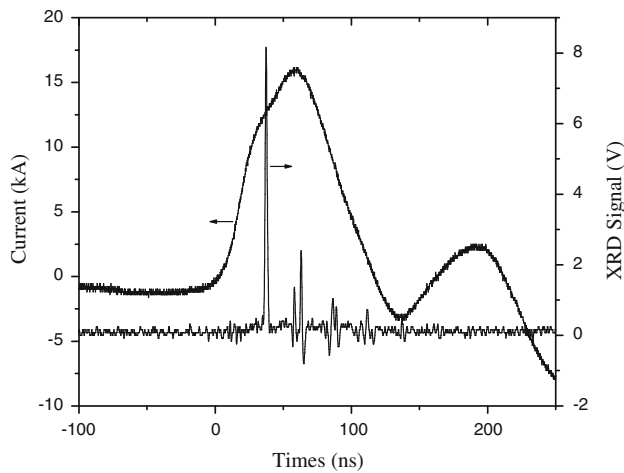
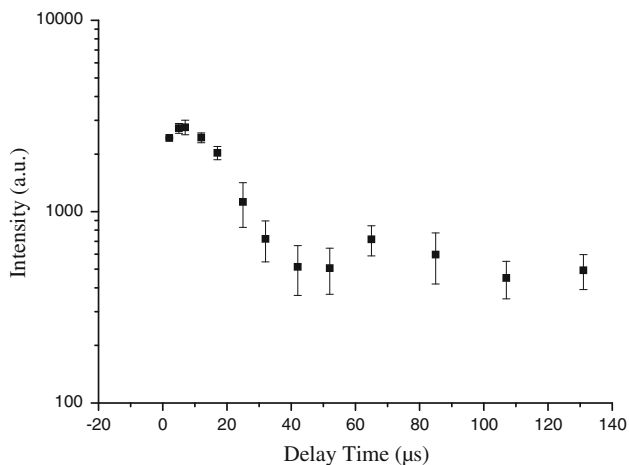**Fig. 5** The waveforms of the main-pulse current and XRD output signal

Fig. 6 46.9 nm lasing intensity under the pre-pulse and main-pulse delay time of 2–130 μs

pressure of Ar gas in capillary is about 17.3 Pa. The results show that the optimum delay time for the laser output is in the region of 2–12 μs. After that, the average amplitude and reproducibility of the laser output decreases until seeing a plateau starting from 52 μs, where the laser output is approximately constant.

To analyze the time-integrated spectrum of the spontaneous radiation from pre-ionized plasma, a visible light Spectrometer was utilized. Figure 7a, b shows the time-integrated spectrum in 420–550 and 650–800 nm, respectively. According to the NIST database [12], the spectral lines of Ar^+, dominate in 420–550 nm, while Ar atom emissions prevail in 665–830 nm. In Fig. 7a, except for the two spectral lines of 426.2 nm (Ar) and 486.1 nm (H_β), all lines are emitted by Ar^+. In Fig. 7b, excluding the strong lines, i.e.: 777.2 nm (O), 777.4 nm (O), and line of 723.6 nm (C^+), the spontaneous radiation of Ar appears to

dominate in the region of 650–800 nm. The spectral lines from H, O and C indicate the existence of a certain amount of H_2O and CO_2 attached on the inner surface of the capillary. However, the H_2O and CO_2 inside the capillary can be neglected, because the spectra from Ar atom and Ar^+ prevail in both spectral regions. In this case, we assumed that the temporal evolution of spontaneous radiation in 420–550 and 650–800 nm can represent the abundance of excited Ar^+ and Ar respectively.

To acquire the temporal evolution of the spontaneous radiation in spectral regions of 420–550 and 650–800, the photodiode and four types of longpass edge filters, which have cutoff wavelengths of 420, 550, 665 and 830 nm, respectively, are utilized in this experiment. The temporal evolution of the spontaneous radiation from Ar^+ ion can be achieved by subtracting the signal of the photodiode with the 550 nm filter from the signal with 420 nm filter. Similarly, the temporal evolution of Ar atom spectrum is obtained with the 830 and 665 nm longpass filter using the same method. The longpass filters utilized in experiments are produced by Union Optic and the part numbers are CFT-GG420-25.4-2, CFT-OG550-25.4-2, CFT-RG665-25.4-2 and CFT-RG830-25.4-2. The temporal evolution of the spontaneous radiation from Ar^+ and Ar in the pre-ionization process has been captured under the same initial pressure and pre-pulse current as Fig. 6. In addition, the signal acquired with the photodiode has good reproducibility during the experiment.

Figure 8 presents the temporal evolution of pre-pulse current, Ar^+ ion and Ar atom emission. As shown in Fig. 8a, pre-pulse voltage breaks through the neutral Ar gas filled in capillary at 0 μs, from which time the pre-pulse current starts. The pre-pulse current jumps instantly to a peak value of 20 A, after that it decays to one-third of the peak value at 66 μs. Figure 8b, c presents the temporal evolutions of spontaneous radiation of Ar^+ ion and Ar atom, respectively. Note that the spike signals before 0 μs are the interfering signals from the breakdown of spark gap in the pre-pulse generating circuit rather than the emission of the pre-ionized plasma. Temporal evolution of emission signal after 0 μs reveals to some extent the information about the kinetic process in the pre-ionization.

As pre-pulse current flows into the capillary, it heats up the Ar gas, and generates pre-ionized plasma accordingly. The increase of the electron temperature and pressure results in the ejection of pre-ionized plasma from the opening end of the capillary. At the same time, the axial flow of gas causes a sound wave in the pre-ionized plasma.

The sound wave and the ejecting effect bring in individually a negative effect on the amplitude of laser: the sound wave propagating along the axis introduces the axial non-uniformity of pre-ionized plasma [8], whereas the ejecting effect causes the reduction of pre-ionized plasma
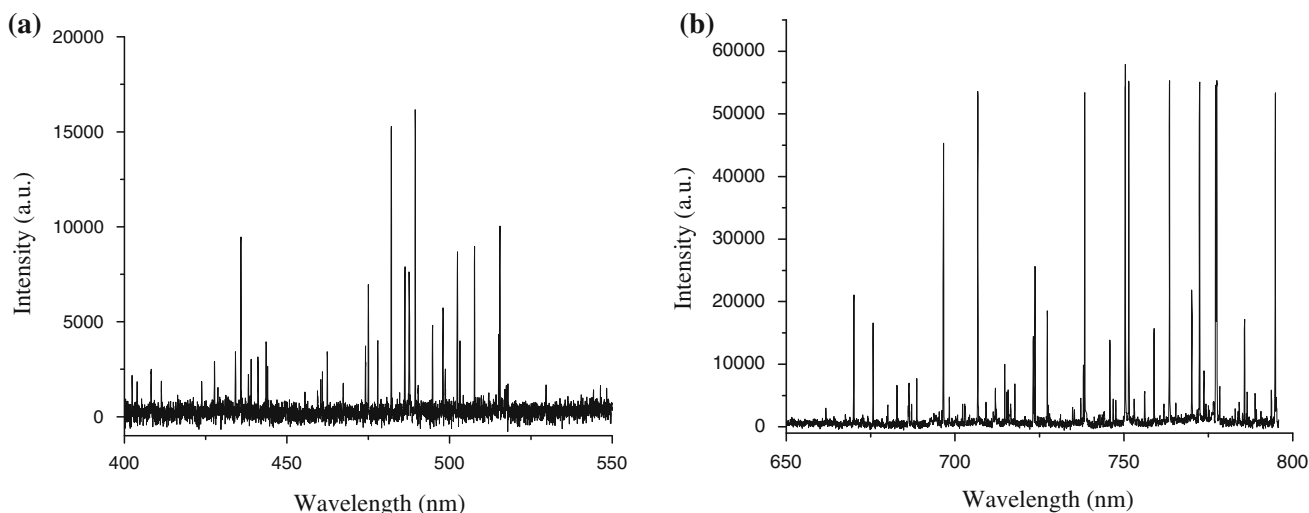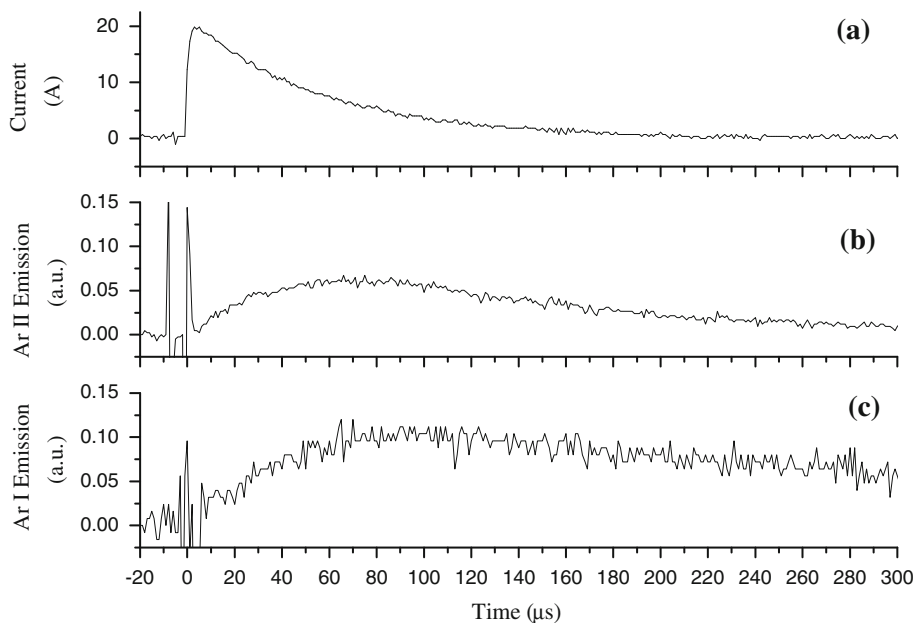
(a)

(b)

Fig. 7 The time-integrated spectrum in **a** 420–550 nm and **b** 650–800 nm

Fig. 8 The temporal evolution of **a** pre-pulse current, **b** Ar$^+$ emission and **c** Ar atom emission

density [10]. The axial non-uniformity of pre-ionized plasma could potentially increase the non-uniformity of laser media formed by the Z-pinch, resulting in the decrease of the amplification of 46.9 nm laser [8]. According to [13], the reduction of pre-ionized plasma density could lead to a overheated plasma formed by Z-pinch, and the resulting high electron temperature diminishes the population inversion between Ne-like Ar $3p$–$3s$ $J = 0$–1 and the gain coefficient of 46.9 nm laser. In other words, the reduction of pre-ionized plasma density could also reduce the amplitude of laser. Therefore, these two existing negative effects are detrimental to the generation of 46.9 nm laser.

The speed of the sound wave propagating inside the plasma, C_s is given by [14]:

$$C_s = \sqrt{\frac{\gamma Z k_B T_e}{m_i}} \tag{1}$$

where Z is the average ionization level, k_B is the Boltzman constant, T_e is the electronic temperature, m_i is the mass of a single ion, and γ is heat capacity ratio, for single element atomic gas, γ is 5/3. An average electron temperature during the pre-ionization process is estimated to be 0.6 eV, which is obtained by the Boltzmann plot method [15] from Ar$^+$ spectral lines as shown in Fig. 7a. By substituting the estimated electron temperature of 0.6 eV and other

corresponding parameters into Eq. 1, one can obtain that the average acoustic speed of pre-ionized plasma is 1.6 mm/μs.

Assuming that the space outside capillary opening end is evacuated, the escape speed of the plasma plume is given by [16]:

$$V_e = \frac{2}{\gamma - 1} C_s \tag{2}$$

Base on this equation, one can easily calculate that the escape speed is 4.8 mm/μs with γ of 5/3 and the acoustic speed of 1.6 mm/μs as derived beforehand.

The influence of pre-pulse and main-pulse delay time on the laser output is analyzed, combining the speeds estimated from Eqs. 1 and 2 with the temporal evolution of Ar^+ ion and Ar atom emission as shown in Fig. 8. During the delay time of 2–12 μs, the amplitude of laser appears to be relatively high and nearly constant as shown in Fig. 6. This can be explained by the fact that the sound wave transmits in a relatively short distance during this time of period, thus the reduction of pre-ionized plasma density can be neglected. In Fig. 8b, c, the increasing intensity of Ar^+ and Ar emission indicates that the electron temperature is less than the average electron temperature of 0.6 eV between 2 and 12 μs. Therefore, the acoustic speed in the capillary is less than the average speed of 1.6 mm/μs. Hence the effective length of the non-uniform pre-ionized plasma column caused by the sound wave is less than 1.9 cm. Comparing with the capillary length of 35 cm, the length of non-uniform plasma column of 1.9 cm with respect to the time period of 2–12 μs is rather short, thus can be considered negligible. Meanwhile, the amount of plasma ejected from capillary is small during this time period, therefore the reduction of pre-ionized plasma density cannot affect the laser output significantly. Base on the above analysis, one can conclude that the influences from the ejecting effect and the axial sound wave on the laser are negligible during the short delay time of 2–12 μs.

As shown in Fig. 6, the amplitude of laser decreases with delay time in the range of 12–52 μs. The decline of lasing intensity at this time period is attributed to the increase of non-uniform pre-ionized plasma length and the reduction of pre-ionized plasma density. Figure 8b, c shows that the intensity of Ar^+ and Ar emission continually increases in 12–52 μs, and nearly reaches the peak value at 52 μs. The growing trend of Ar^+ and Ar emission indicates that the pre-pulse current is continuously heating the plasma. The sound wave is propagating along the capillary with the average acoustic speed of 1.6 mm/μs. Therefore, a length of the pre-ionized plasma up to 8.3 cm is affected by 52 μs, which is approximately 1/4 of the length of the 35 cm capillary. As a result, the amplitude of laser is decreasing severely with the delay time of 12–52 μs. At the

same time, a large amount of pre-ionized plasma is ejected from the capillary with an average speed of 4.8 mm/μs, leading to a drastic drop of pre-ionized plasma density, which brings down the intensity of laser accordingly. In conclusion, the drastic drop of lasing intensity between 12 and 52 μs is due to the axial non-uniformity plasma formed by the propagation of the sound wave, and the density reduction of pre-ionized plasma caused by the ejecting effect.

4 Conclusion

Lasing of Ne-like Ar 46.9 nm pumped by capillary discharge is observed under pre-pulse and main-pulse delay time of 2–130 μs. The influence of the delay time on the laser intensity is studied with the temporal evolution associated with the time-integrated spectrum of the spontaneous radiation from pre-ionized plasma. We believe that the severe decrease of lasing intensity with delay time above 12 μs is due to the density reduction caused by the ejecting effect, and the axial non-uniformity of the Ar pre-ionized plasma due to the axial sound wave. Thus, high laser output intensity cannot be obtained with the delay time more than several tens of microsecond.

References

1. J.J. Rocca, V. Shlyaptsev, F.G. Tomasel, O.D. Cortázar, D. Hartshorn, J.L.A. Chilla, Phys. Rev. Lett. **73**(16), 2192 (1994)
2. J. Filevich, K. Kanizay, M.C. Marconi, J.L.A. Chilla, J.J. Rocca, Opt. Lett. **25**, 356 (2000)
3. J.J. Rocca, E.C. Hammarsten, E. Jankowska, J. Filevich, M.C. Marconi, S. Moon, V.N. Shlyaptsev, Phys. Plasmas **10**, 2031 (2003)
4. B.R. Benware, A. Ozols, J.J. Rocca, I.A. Artioukov, V.V. Kondratenko, A.V. Vinogradov, Opt. Lett. **24**, 1714 (1999)
5. C.A. Brewer, F. Brizuela, D. Martz, G. Vaschenko, M.C. Marconi, J.J. Rocca, C.S. Menoni, Soft X-Ray Lasers and Applications VII. **6702**, 67020M (2007)
6. A. Ben-Kish, M. Shuker, R.A. Nemirovsky, A. Fisher, A. Ron, J.L. Schwob, Phys. Rev. Lett. **87**, 015002 (2001)
7. Y. Hayashi, Y. Xiao, N. Sakamoto, H. Miyahara, G. Niimi, M. Watanabe, A. Okino, K. Horioka, E. Hotta, Jpn. J. Appl. Phys. **42**, 5285 (2003)
8. M. Shuker, A. Ben-kish, R.A. Nemirovsky, A. Fisher, A. Ron, Phys. Plasmas **13**, 013102 (2006)
9. G. Tomassetti, A. Ritucci, A. Reale, L. Palladino, L. Reale, S.V. Kukhlevsky, F. Flora, L. Mezi, J. Kaiser, A. Faenov, T. Pikuz, Eur. Phys. J. D **19**, 73 (2002)
10. C.A. Tan, K.H. Kwek, Phys. Rev. A **75**, 043808 (2007)
11. Y. Zhao, Y. Cheng, B. Luan, Y. Wu, Q. Wang, J. Phys. D Appl. Phys. **39**, 342 (2006)

12. NIST atomic spectra database: http://www.physics.nist.gov/PhysRefData/ASD/index.html (2011)
13. Y.P. Zhao, S. Jiang, Y. Xie, Q. Wang, Appl. Phys. B **99**, 535 (2010)
14. J.D. Huba, *NRL Plasma Formulary* (The Office of Naval Research, Washington D.C., 1998)
15. N.M. Shaikh, Y. Tao, R.A. Burdt, S. Yuspeh, N. Amin, M.S. Tillack., J. Phys.: Conf. Ser. 244 042005 (2010)
16. Y.B. Zel'dovich, Y.P. Raizer: Physics of Shock Waves and High-Temperature Hydrodynamic Phenomena (Dover Publications Inc., New York, 2002)